Journal of Materials and Environmental Science
ISSN : 2028-2508
e-ISSN : 2737-890X
CODEN : JMESCN

J. Mater. Environ. Sci., 2023, Volume 14, Issue 9, Page 1078-1095

http://www.jmaterenvironsci.com

Reduction of the corrosive character of a biogas: elimination of hydrogen sulfide by filtration on activated carbon based on palm kernel shell

Ahissan Donatien EHOUMAN [1]*, Adjoumani Rodrigue KOUAKOU [1], Mohamed COULIBALY [2], Gbangbo Remis KONAN [3], Amara BAMBA [2], Paulin Marius NIAMIEN [2], Benjamin YAO [3,4]

[1]*Laboratoire de Thermodynamique et Physico-Chimie du Milieu, Université NANGUI ABROGOUA, Abidjan 02, Côte d'Ivoire.*

[2]*Laboratoire de Réaction et Constitution de la Matière, Université Félix Houphouët Boigny, Abidjan 22, Côte d'Ivoire*

[3]*École Doctorale Polytechnique, Institut National Polytechnique Félix Houphouët-Boigny, Yamoussoukro, Côte d'Ivoire*

[4]*Centre d'Excellence Africain Pour la Valorisation des Déchets en Produits À Haute Valeur Ajoutée (CEA-VALOPRO), Institut National Polytechnique Félix Houphouët-Boigny (INP-HB), BP 1093, Yamoussoukro, Côte d'Ivoire.*

Corresponding author : ehoumandona@gmail.com

Received *20 July 2023,*
Revised *02 Sept 2023,*
Accepted *05 Sept 2023*

Citation*: Ehouman A. D., Kouakou A. R., Coubaly M., Konan G. R., Bamba A., Niamien P. M., Yao B. (2023) Reduction of the corrosive character of a biogas: elimination of hydrogen sulfide by filtration on activated carbon based on palm kernel shell, J. Mater. Environ. Sci., 14(9), 1078-1095*

Abstract: Biogas is a gas that contains mainly CO_2 and methane, and hydrogen sulfide (H_2S) in trace amounts. H_2S is a dangerous gas that corrodes metals used in anaerobic digestion and also in the petrochemical industry, etc. The objective of this work is to study the performance of an activated carbon prepared from palm kernel shell in the removal of hydrogen sulfide (H_2S) from biogas and to evaluate the reduction of the corrosive effect of filtered biogas on Al and Cu metals. The impregnation and carbonization method was used for the preparation of activated carbon based on palm kernel shell and the gravimetric method for the study of the corrosion rate of Al and Cu metals in biogas. The results indicate that the prepared activated carbon is microporous, of good quality and lightweight. Furthermore, the prepared activated carbon samples have removal efficiency (RE) greater than 90% of H_2S. The values of induced protective power in the case of aluminum and copper in the filtered biogas are 82.63% and 85.47%, respectively. Contact time can be considered to increase the removal rate.

Keywords: *Biogas; Copper; Corrosion; Mass loss*

1. Introduction

Ivory Coast, a country located in West Africa, aims to be the energy leader in Sub-Saharan Africa over the next twenty years. To achieve this goal, the Ministry of Petroleum, Energy and Renewable Energies needs to intensify the exploitation of mining and energy resources, with a view to turning these sectors into real industrial hubs, while making energy abundant, high-quality and inexpensive to accelerate the country's economic and social development (Tsassa, 2015).

Biogas production is one of the most important ways of producing clean energy, and of coupling this production with the management and treatment of waste and its degradation by-products (El houari, 2018). In this way, biogas represents both an energy and an environmental solution resulting from a

sustainable process (Nyamukamba *et al,* 2022). It encompasses a wide variety of gases produced by specific treatment processes, from organic waste of industrial, animal, household or other origin. It is a gas that mainly contains combustible methane (CH_4) and carbon dioxide (CO_2), but also contains other elements such as trace amounts of hydrogen sulfide (H_2S) (Kougias *et al.,* 2018). Hydrogen sulfide is a highly odorous, toxic and corrosive compound (Abdirakhimov *et al.,* 2022; El Mouaden *et al.,* 2018). It inhibits methanogenic bacteria, which in turn reduces the concentration of methane in the biogas (Kaiser *et al.,* 2004). Hydrogen sulfide has also been identified as one of the main causes of corrosion failure in the gas and petrochemical industries (Nikiema *et al.,* 2015). It can considerably reduce the useful life of transport pipelines and processing plants in the oil and gas industry through cracking (Asmara, 2018, Sun *et al.,* 2010). With this in mind, its elimination from biogas is becoming a technical, environmental and health imperative. It is therefore essential to consider the treatment of H_2S from biogas using local, available and inexpensive materials. There are several industrial H_2S purification methods based on chemical, physical or biological principles, more specifically biological desulfurization, membrane principles, adsorption on adsorbent materials, etc. (Sawalha *et al.,* 2020). Like the other methods, adsorption on activated carbon offers several advantages. Indeed, its use is recognized as a less costly method, offering the possibility of saving 50% of the cost of its production when regenerated (Demey et al., 2018). In addition, the use of activated carbon offers significant efficiency in the elimination of pollutants through high-performance adsorbents (Benhamed et al., 2015, Benhamed et al., 2018). As Côte d'Ivoire is an agricultural country, the purification of hydrogen sulfide requires the use of locally available and inexpensive materials. Several studies have focused on the use of activated carbon as an adsorbent material for H_2S adsorption (shang et al., 2016, Ehouman et al., 2023, Gbangbo et al., 2023). For this reason, palm kernel shell, which is accessible and also available in large quantities in national territory was chosen.

2. Materials and methods

2.1 Materials

As a precursor, we used dried and pounded palm kernel shells, as Côte d'Ivoire is the second largest producer of African diet, with 1,800,000 tonnes per year. It occupies this position just after Nigeria, with which it accounts for most of the 4% of the world market supplied by Africa. Its abundance and accessibility in several regions of the country have therefore prompted its use in the manufacture of activated carbon. **Figure 1** below shows the shell of dried palm kernels.

Figure 1: Raw material for activated carbon production

The study metals used, aluminum and copper, were pre-treated and oven-dried at 40°C for 5 min before being transported to the experimental biogas site. **Figure 2** below shows the copper and aluminum samples.

Figure 2: Aluminum(c) and Copper (d)

The necessary mass measurements of our material and of the copper and aluminum samples for the various manipulations were carried out using balances (**Figure 3**).

Figure 3: OHAUS precision balance

For sieving the precursor (palm kernel shell) crushed using the mortar below, we used 8 mm and 4 mm porosity sieves, one example of which is illustrated in **Figure 4 and Figure 5** below:

Figure 4: Mortar

Figure 5: Sieve

An oven was used to dry the palm kernel shells and activated charcoal for 24 hours. The palm kernel shells were carbonized using an electric furnace, as shown in **Figure 6** and **Figure 7** below:

Figure 6: Drying oven

Figure 7: Electric oven

A stirrer was used to agitate the charcoal-iodine mixture during iodine value determination (**Figure 8**). A pH meter was used to measure the pH of the water used to wash our carbon, to ensure that it was close to 7 (**Figure 9**). H_2S concentration is determined using a portable biogas detector (**Figure 10**).

Figure 8: Magnetic stirrer

Figure 9: pH meter

Figure 10: Biogas analyzer

2.2 METHODS

2.2.1. Protocol for preparing 20% phosphoric acid (H_3PO_4)

The phosphoric acid stock solution used has a purity of 85%, a molar mass of 98 g/mol and an initial concentration C_0 =14.65 mol/L. The final concentration C_f of the 20% phosphoric acid solution (daughter solution) is determined by **Eqn. 1:**

$$C_f = \frac{x \times ds \times \rho eau}{M} \qquad \textbf{Eqn. 1}$$

x: percentage of daughter solution

ds: density of the phosphoric acid solution as a function of percentage. According to the CSTP at 20%, ds = 1.1134

ρwater: density of water, ρwater = 1000 g/L

M: Molar mass of H_3PO_4 solution

M = 98 g/mol

The initial volume of the stock solution to be taken is expressed with **Eqn. 2**:

$$Vo = \frac{Vf \times Cf}{Co} \qquad \textbf{Eqn. 2}$$

with Vf = 1000 ml. Using a graduated cylinder, we measure a volume V_0 =155 ml of the phosphoric acid stock solution, which we place in a 1-liter volumetric flask containing distilled water and fill to the mark.

2.2.2. Activated carbon synthesis protocol

Good quality activated carbons with a very large pore structure and high specific surface area are prepared from plant biomasses using ortho-phosphoric acid as the activating agent (Laine et al., 1989, Hu et al., 1999, Prahas et al., 2008). In the case of our study, activated carbon was synthesized from palm kernel shells using the chemical activation method. In a closed glass jar, 50 g of palm kernel hull is impregnated in 290 ml of H_3PO_4 daughter solution for 24 h. After the impregnation time, the carbon is chemically activated. After the impregnation time, we place the impregnated precursor in the oven to dry for 24h at 105°C (Koné et al., 2021) . This is followed by the activation phase.

The precursor, already impregnated and dried in the oven, is placed in a porcelain container and then carbonized in the electric furnace at a given temperature and time; in our case at 550°C for 3h47min (Abuiboto et al., 2016). The samples are then washed out of the oven, while the pH of the rinsing water is measured. Once the pH of the water is close to 7, the washed samples are oven-dried for 24h at 105°C.

2.2.3 Characterization

- Yield

Overall, activated carbon preparation yields are higher at 400°C than at 600°C, irrespective of activated carbon size. Yield is a function of carbonization time and temperature. Yield is the ratio between the quantity of precursor and the quantity of activated carbon prepared. We measure a quantity of precursor which we carbonize (m_0), and at the furnace outlet we measure the quantity of carbon produced (m_1). The yield (%) is given by **Eqn. 3**:

$$R\ (\%) = [(m_1 / m_0)] \times 100 \quad (3) \qquad \textbf{Eqn. 3}$$

- Iodine value

The iodine index test is designed to determine carbon's ability to adsorb small molecules. It characterizes the micropores accessible to small particles. The iodine index is an important characteristic in the evaluation of activated carbon micropores. It was determined as follows. A 15 ml volume of 0.1 N iodine solution is brought into contact with 0.05 g activated carbon for 4 min. The treated solution was filtered, then 10 ml of filtrate was assayed with a 0.1 N sodium thiosulfate solution in the presence of a few drops of a 0.1 N starch starch solution used as a color indicator. The sodium thiosulfate solution was added little by little to the Erlenmeyer flask containing the filtrate, until the solution was completely discolored. A blank test was carried out under the same conditions in the absence of activated carbon, giving a volume V_b = 5.4 ml (Adjoumani, 2022a, Adjoumani, 2022b). Finally, the iodine value (Id) expressed in mg/g was calculated by **Eqn. 4**:

$$\text{Iodine value (Id) (mg/g)} : \mathbf{I_d} = \frac{(\mathbf{V_b - V_s}) \times \mathbf{N} \times \mathbf{126{,}9} \times (\frac{\mathbf{15}}{\mathbf{10}})}{\mathbf{m}} \qquad \textbf{Eqn. 4}$$

With :
Vb: volume in ml of 0.1 N sodium thiosulfate added to the blank test.
Vs: volume in ml of 0.1 N sodium thiosulfate added to the adsorbent test.
N: normality of sodium thiosulfate solution in (eq.g/L).
126.9: atomic mass of iodine.
m: mass of adsorbent in (g).

- Ash content Tc

The ash content indicates the richness of the material in minerals such as silica, aluminum, iron, magnesium and calcium. The result is expressed as a percentage of ash content on dry coal (ash mass / dry fuel mass). To determine this, we used the following method:

Firstly, 0.5 g of activated charcoal was placed in a crucible and placed in an oven at 80°C for 24 hours. Then, after drying, the crucible and its contents were placed in an oven set at 650°C for 3 h. After cooling to room temperature, the crucible and its contents were weighed again (Kone et al., 2022). The ash content (Tc) was determined by **Eqn. 5**:

$$Tc\ (\%) = [(m_3 - m_2) / m_1] \times 100 \qquad \textbf{Eqn. 5}$$

m_1: mass of coal ;
m_2: mass of crucible and coal after removal from furnace;
m_3 : mass of crucible and coal after drying.

2.2.4 Test of H_2S removal by adsorption on activated carbons

Biogas sampling was carried out at the FONDATION BRIN poultry farm, located in the village of YAOKOKOROKO, sub-prefecture of TABAGNE in the GONTOUGO region (Côte d'Ivoire). This farm has a methanizer with a capacity of 15 m^3 for processing hen droppings (poultry waste). **Figure 11** below shows the methanizer:

Figure 11: Overview of the BRIN FOUNDATION Methanizer

1: Methanizer; 2: Manual feed tank; 3: Automatic feed tank;
4: Outlet; 5: Methanization digestate tank (liquid & solid fraction); 6: Biogas filtration and purification system; 7: Temperature sensors (digester and digestate).

- Method for determining removal efficiency (RE)

H_2S concentration is determined at the inlet and outlet of the filter column using a portable biogas detector. For the duration of the test, the biogas flow rate was kept constant at 0.146 m^3/min so (0.00244 m^3/s). **Figure 12** below shows the adsorption test setup.

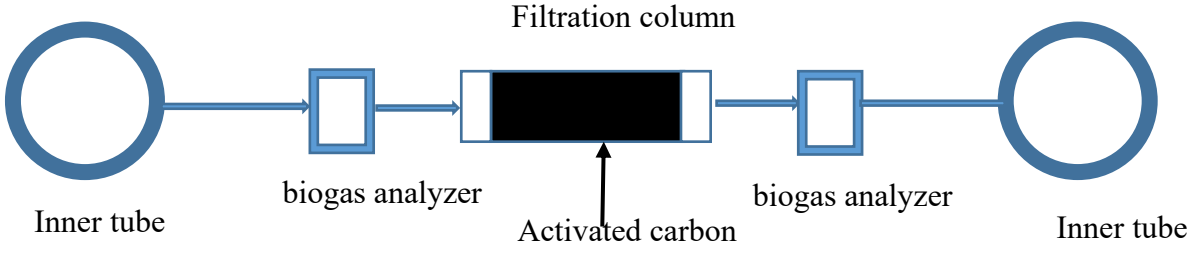

Figure 12: Adsorption test diagram

Elimination efficiency (RE) was calculated using **Eqn. 6** below:

$$RE = \frac{Ci-C}{Ci} \times 100 \quad \textbf{Eqn. 6}$$

Where Ci and C are the initial and final H_2S concentrations (Adjoumani, 2022a, Adjoumani, 2022b)

2.2.5 Gravimetry

Mass loss is the oldest method for measuring corrosion. It is based on the determination of the corrosion rate. It is a simple method, the principle of which is to immerse the surface sample (S) to be studied in the corrosive medium in question (after weighing it) for a well-defined period of time (t) [25]. Then, after washing, the sample is weighed again to determine the mass loss (Δm) **(Eqn. 7)**.

$$\Delta m = m_0 - m_1 \quad \textbf{Eqn. 7}$$

m_0: Initial sample mass (g)
m_1: Final sample mass (g)
Δm: mass loss (g).

2.2.5.1 Experimental protocol

Gravimetry is an experimental method for monitoring the evolution of the mass of a sample immersed in a corrosive medium over time. The experimental procedure for this method in our case is as follows:

- Place the sample in the biogas contained in an air chamber after weighing it, i.e. m1 (**Figure 13**).
- Remove the sample after 5 hours, 24 hours, 48 hours and 72 hours.
- Wash the sample thoroughly with distilled water and clean with a brush.
- Dry it in an oven and weigh it again, i.e. m^2 the new mass.

Figure 13: Air chambers containing biogas and samples

The corrosion rate value is the average of three tests carried out under the same conditions. The studies were carried out with several samples of each metal of different masses placed in an air chamber containing biogas for 5H, 24H, 48H and 72H.

The average corrosion rate of copper (W) was determined by mass loss **(Eqn. 8)**

$$W = \frac{\Delta m}{S.t} [mg.cm^{-2}\ h^{-1}] \quad \textbf{Eqn. 8}$$

With :
Δm: mass loss (in g) ;
S: total surface area of the sample (in cm2) ;
t: immersion time (in h).

3. Results and discussion

3.1 Characterization of palm kernel shell activated carbon (CACGP)

The study of the characteristics of activated carbons is necessary to contribute to the understanding of several phenomena such as adsorption, desorption, exchange, etc. **Table 1** below shows some of the characteristics of the prepared activated carbon (CACGP).

Table 1: Activated carbon characteristics

	Iodine value (mg /g)	Yield (%)	Ash content (%)	pH
CACGP	818,505	41	4,36	5

3.1.1 Iodine value

Activated carbon contains pores accessible to iodine molecules. The iodine value is 818.505 mg/g. The higher the iodine value, the more microporous the adsorbent (0-2 mm) and the better its specific surface area. In the case of our study, palm kernel shell activated carbon (CACGP) activated with phosphoric acid shows better results (values above 500 mg/g) (Rodrigue et al., 2022, Koné et al., 2022, Frank, 2012, Ehouman et al., 2023, Balogoun et al., 2015).

3.1.2. Yield

Activated carbon yield is an important measure of the feasibility of producing activated carbon from a given precursor under given conditions. In the case of our study, the yield of activated carbon prepared from palm kernel shell (CACGP) obtained is 41%. This shows a good yield, as it exceeds 20% (Balogoun et al., 2015).

3.1.3. Ash content

Ash content is one of the parameters influencing the adsorption properties of carbon. This parameter has a significant effect on activated carbon quality. It appears that a high ash content reduces the specific surface area. On the other hand, the ash content of a good adsorbent should not be too high, i.e. below 20% (Coelho et al., 2006). An excessively high ash content (>20%) reduces the carbon's activity and reactivation potential, and can lead to leakage of impurities (mineral salts). In our study, the ash content of activated carbon prepared from palm kernel shells (CACGP) was 4.36%. The ash content obtained in this study shows a very good adsorption capacity of the synthesized activated carbon (Rodrigue et al., 2022).

3.2 Study of the efficiency of hydrogen sulfide removal from biogas by palm kernel shell activated carbon (CACGP)

3.2.1 Biogas composition

The plant system is equipped with a methanizer that produces biogas composed of methane (CH_4), carbon dioxide (CO_2), carbon monoxide (CO) and hydrogen sulfide (H_2S). Changes in H_2S concentration prior to adsorption were also monitored during the working time and showed no change in the initial H_2S concentration (**Table 2**). This means that the initial H_2S concentration remained constant during the working time.

Table 2: Biogas composition

Components	Measure 1	Measure 2	Measure 3	Measure 4
CH_4	85-90 %	85-90 %	85-90 %	85-90 %
CO	10-15 ppm	85-90 ppm	85-90 ppm	85-90 ppm
H_2S	80 – 100 ppm	80 – 100 ppm	80 – 100 ppm	80 – 100 ppm

3.2.2 Removal of hydrogen sulfide (H_2S) from biogas

CACGP was used to remove hydrogen sulfide (H_2S) from biogas. **Figure 14** below shows H_2S concentrations at the outlet of 30 g CACGP in the filtration column as a function of time. Using a mass of 30 g, which is the maximum amount of activated carbon the filter can hold, we observe that at the start of filtration, the H_2S concentration is zero and increases progressively until it reaches a concentration of 6.35 ppmV after 140 min. This concentration remained constant up to 600 minutes (10 hours) **Figure 15**. The very low value observed (2 ppmv) at the start of filtration could be explained by the highly porous nature of our activated carbon. The gradual increase in H_2S concentration over time may be due to the occupation of adsorption sites by H_2S molecules. However, concentrations remained below 10 ppmV, the threshold concentration for prolonged exposure or the 8-hour exposure limit value (Moletta, 2011). These concentrations are also below 16 ppmV, which is indicated to minimize the impact of biogas on storage, compression and transport equipment for valorization in free compressor units (Promnuan *et al.*, 2017).

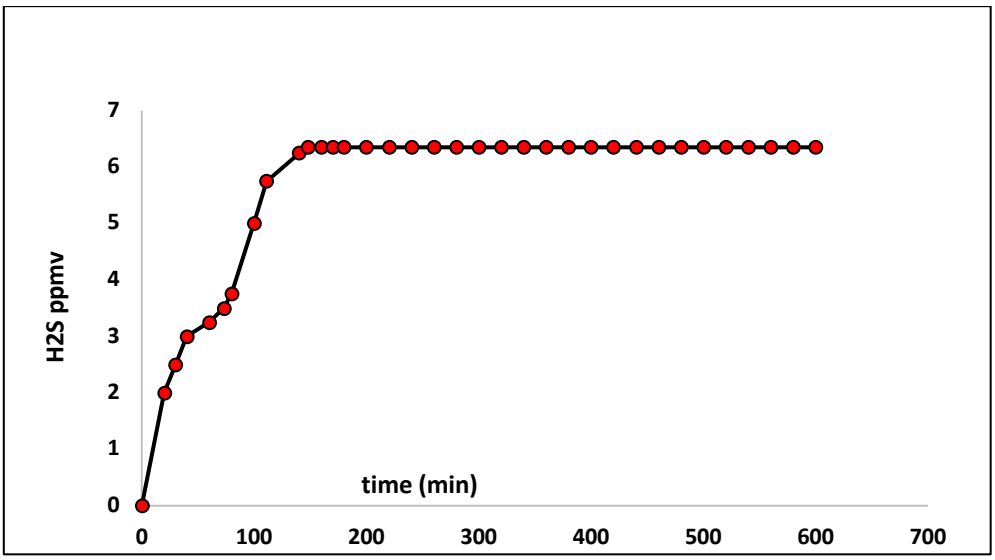

Figure 14: Variation in H_2S concentration as a function of time for a CACGP mass of 30 g

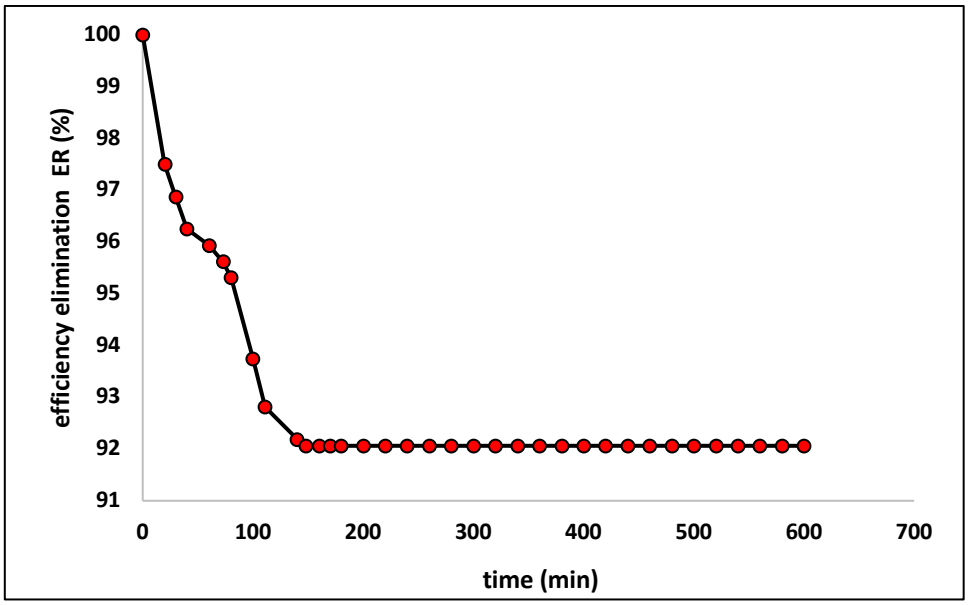

Figure 15: H_2S removal efficiency (RE) versus time for a CACGP mass of 30 g

It should be noted that the CACGP did not reach breakthrough time within the working time (10 hours). It should be remembered that breakthrough time is the time at which the H_2S concentration at the exit of the filtration column becomes half the initial concentration, i.e. between 40-50 ppm in the case of our experiment. Furthermore, the CACGP has a very high H_2S removal efficiency (RE) of 92.06% over 10 hours (**Figure 15**). This would indicate the development of the pores essential for adsorption (Promnuan *et al.,* 2017, Mao *et al.,* 2021).

3.3 Study of aluminum and copper corrosion in biogas

3.3.1 Evaluation of mass loss of aluminum (Al) and copper (Cu) as a function of time (t)

3.3.1.1 Evaluation of aluminum (Al) mass loss as a function of time (t)

Figures 16 below show a comparison of aluminum mass loss in unfiltered biogas (BNF) and filtered biogas (BF). The various **Figures 16,** above, clearly show an increasing trend in mass loss with increasing time for the aluminum metal used in the case of unfiltered biogas (BNF) and in filtered biogas (BF). A greater mass loss is also observed in the different cases with the longer exposure time of 72 hours in the case of our study. For unfiltered biogas, the increasing trend is higher than for filtered biogas. This could be explained by the presence of hydrogen sulfide (H_2S) in very high concentrations of 90 ppm in unfiltered biogas and 6.35 ppm in filtered biogas. Hydrogen sulfide therefore has a corrosive effect on aluminum.

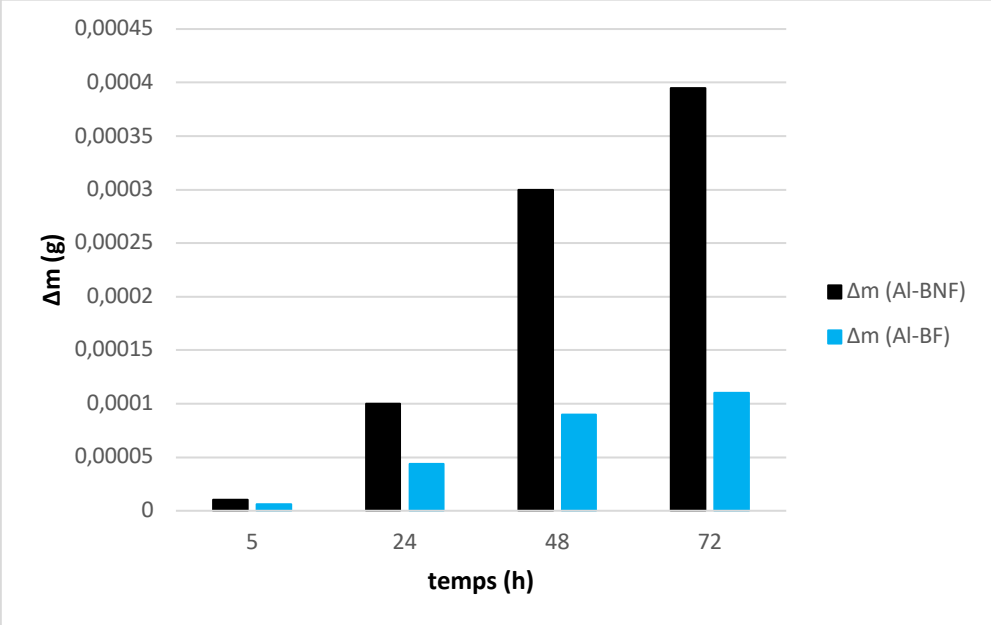

Figure 16: Mass loss of aluminum in unfiltered biogas (BNF) and in filtered biogas (BF).

A direct assessment of **Figure 16** shows that aluminum is more sensitive to weight loss when exposed to direct contact with unfiltered biogas (BNF) than with filtered biogas (BF). In fact, in BNF the corrosion process is higher. This could be explained by the high H2S concentration and high moisture content, which are factors that favor corrosion. On the other hand, in BF, the corrosion process exists, but is slowed down. The slowdown in aluminum corrosion in BF could be explained firstly by the low H_2S content, and secondly by the low water content, due to the adsorption of water and H_2S molecules by the activated carbon during filtration. This would indicate the formation of a surface layer acting as a protective layer, preventing the propagation of the corrosion process in our metal (Fontenelle *et al.,* 2017).

3.3.1.2 Evaluation of copper (Cu) mass loss as a function of time (t)

Figure 17 below shows a comparison of copper mass loss in unfiltered biogas (BNF) and filtered biogas (BF). A direct evaluation of the different figures indicates that copper has a greater mass loss when exposed for longer periods (72h) to direct contact with unfiltered biogas. For filtered biogas, an increasing trend towards mass loss with increasing time is also observed. This increasing trend in mass loss with increasing time observed in both cases (BNF and BF) could reflect a sensitivity to copper corrosion by hydrogen sulfide (H2S) contained in the biogas at concentrations of 90 ppm and 6.35 ppm.

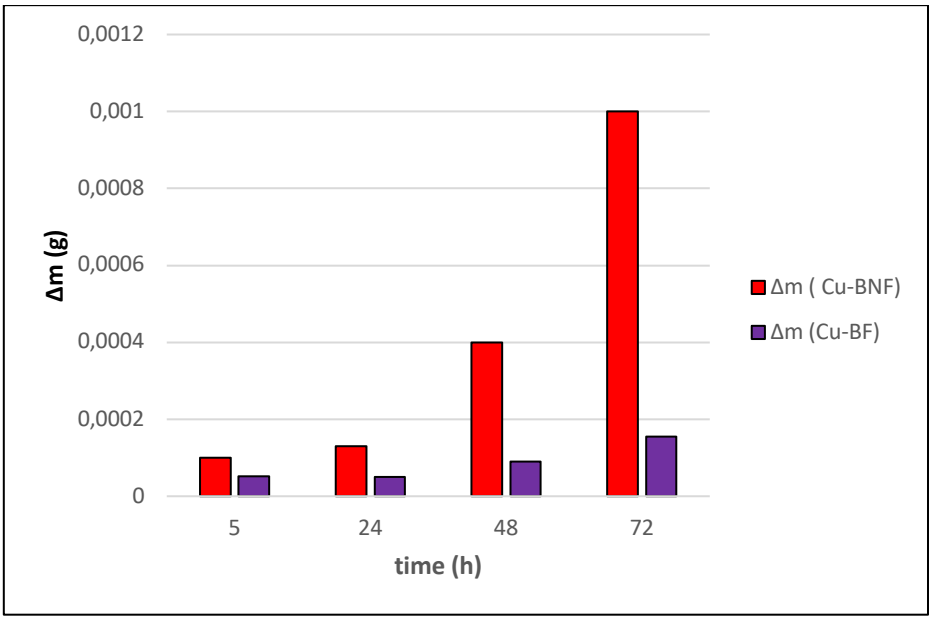

Figure 17: Copper mass loss as a function of time in unfiltered biogas (BNF) and filtered biogas (BF).

Comparison of the evaluation of copper mass loss as a function of time in BNF and BF (17), indicates that copper has a high sensitivity to mass loss, particularly when directly exposed to BNF. Clearly, mass losses are greater when copper is directly exposed to BNF biogas than in BF. Indeed, in BNF the material is exposed to high H_2S concentrations (90 ppm) as well as to the high moisture content contained in BNF. This could accelerate the corrosion process, resulting in significant mass loss.
The observed slowdown in copper corrosion on contact with BF could be explained not only by the low H2S (6.35 ppm) and moisture contents due to adsorption of water molecules by the activated carbon during filtration, but also by the formation of a layer acting as a protective barrier, preventing the propagation of the corrosion process of the metal used (Fontenelle *et al.,* 2017).

3.3.2 Study of the corrosion rate of the metals aluminum (Al) and copper (Cu) as a function of time (t) in biogas

3.3.2.1 Study of aluminum (Al) corrosion rate as a function of time (t) in biogas

The most appropriate way to interpret the corrosion process is through the corrosion rate or corrosion speed. This parameter indicates whether the corrosion process is stable (with a constant corrosion rate), more aggressive (with a higher corrosion rate) or milder with (decreasing corrosion rate) (Dustin, 1934, Fontenelle *et al.,* 2017). A process with a corrosion rate equal to or close to zero indicates that the corrosion process is inactive (Dustin, 1934, Fontenelle et al., 2017). Figure18 below shows the variation in aluminum corrosion rate as a function of time in unfiltered biogas (control) and

in biogas filtered by CACGP activated carbon. Analysis of this figure shows that the corrosion rate increases with study time in the case of aluminum (control), i.e. In unfiltered biogas (BNF). The high corrosion rate, characterized by increasing mass loss, indicates a more aggressive corrosion process (Dustin, 1934). This could be explained by the continuous loss of the element aluminum (Al) due to its weakening as a result of the high concentration of moisture and hydrogen sulfide H_2S present in its immediate environment. On the other hand, with aluminum in the presence of filtered biogas (BF), the curve of the evolution of the corrosion rate as a function of time has, on the whole, a decreasing tendency over time. In this case, the curve shows a milder corrosion process during the contact time up to 72h [37-38]. This could be explained by the presence of trace amounts of CACGP-based activated carbon **(Figure 18)**.

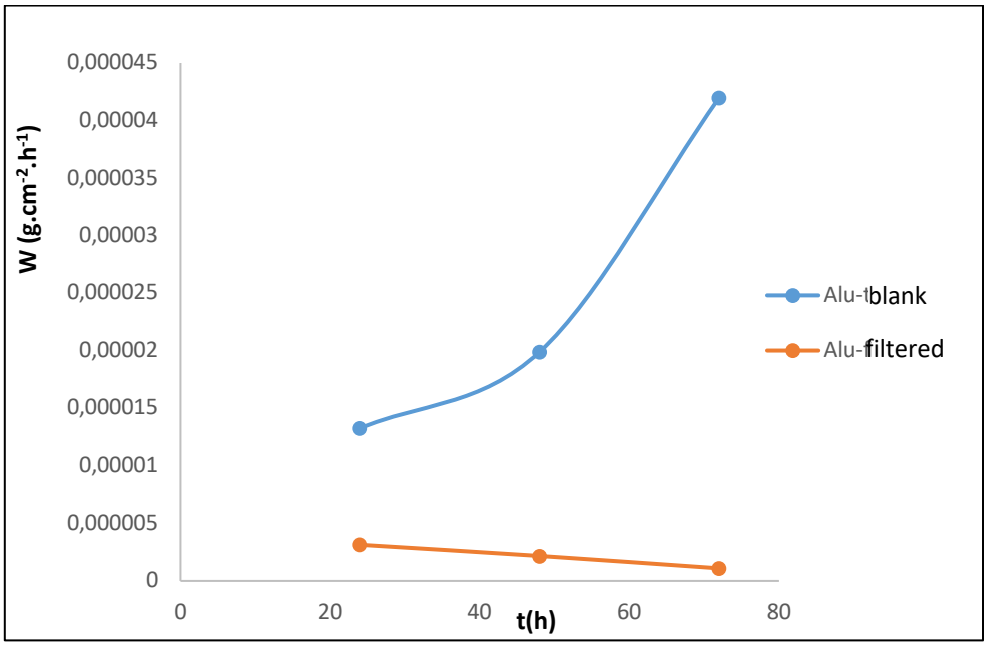

Figure 18: Evolution of aluminum corrosion rate as a function of time in unfiltered biogas (control) and in biogas filtered (BF) by CACGP activated carbon.

3.3.2.2 Study of copper (Cu) corrosion rate as a function of time (t) in biogas

Figure 19 below shows the variation in copper corrosion rate as a function of time in unfiltered biogas (control) and in biogas filtered (BF) with CACGP activated carbon. In BNF, an increase in copper corrosion rate was observed with increasing biogas contact time. The increase in the corrosion rate of copper exposed to BNF, could be explained by the continuous loss of Cu element and the consequent weakening of the copper metal structure due to the acidic environment present in BNF due to its high H_2S concentration and high moisture content (Search, and Out, 2012, Ali, 2021). The decrease in the corrosion rate of aluminum exposed to BF up to 48 h visible in the figure, reflects a low loss of Cu element mass. This low mass loss is thought to be due to the inhibitory effect of activated carbon based on palm kernel shells. In fact, the high H2S and water contents responsible for accelerating the rate of corrosion were reduced in the BF by the traces of activated carbon forming a protective physical barrier for our metal. However, we observed a slightly modified trend after 48 h up to 72 h, showing a minor increase in corrosion rate, relative to time. This could be explained by the metal's sensitivity to mass loss due to the low H_2S content, which influences the hardness of our metal's crystalline surface (Search, and Out, 2012, Ali, 2021). Overall, however, the corrosion rate in BNF is higher than in BF.

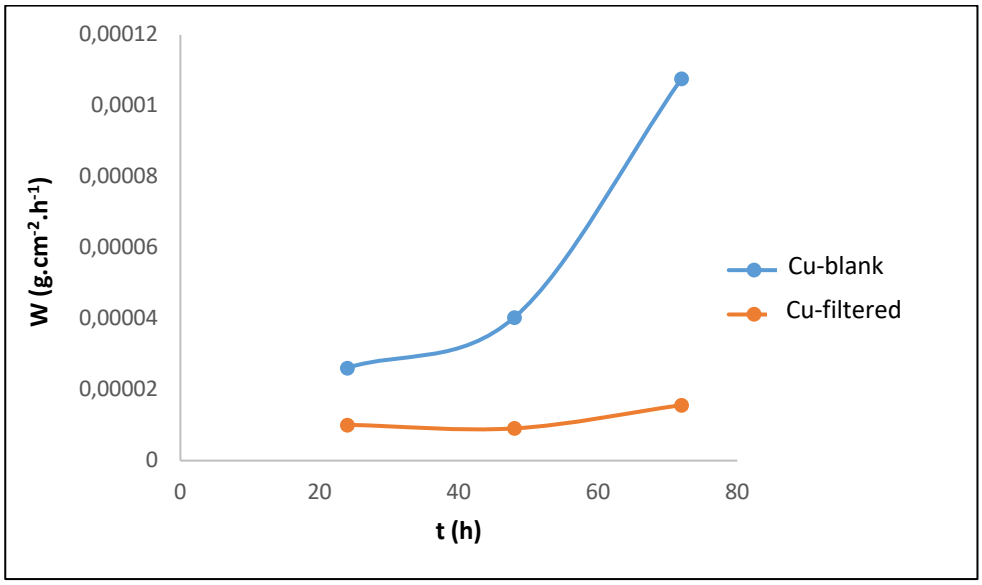

Figure 19: Copper corrosion rate as a function of time in unfiltered biogas (BNF) and in biogas filtered (BF) with CACGP activated carbon.

3.3.3 Comparative study of the corrosion rate of aluminum and copper (Cu) as a function of time (t) in biogas.

3.3.3.1 Comparative study of aluminum and copper (Cu) corrosion rates as a function of time (t) in unfiltered biogas (BNF)

Figure 20 below shows the variation of aluminum and copper corrosion rates as a function of time in unfiltered biogas (control).

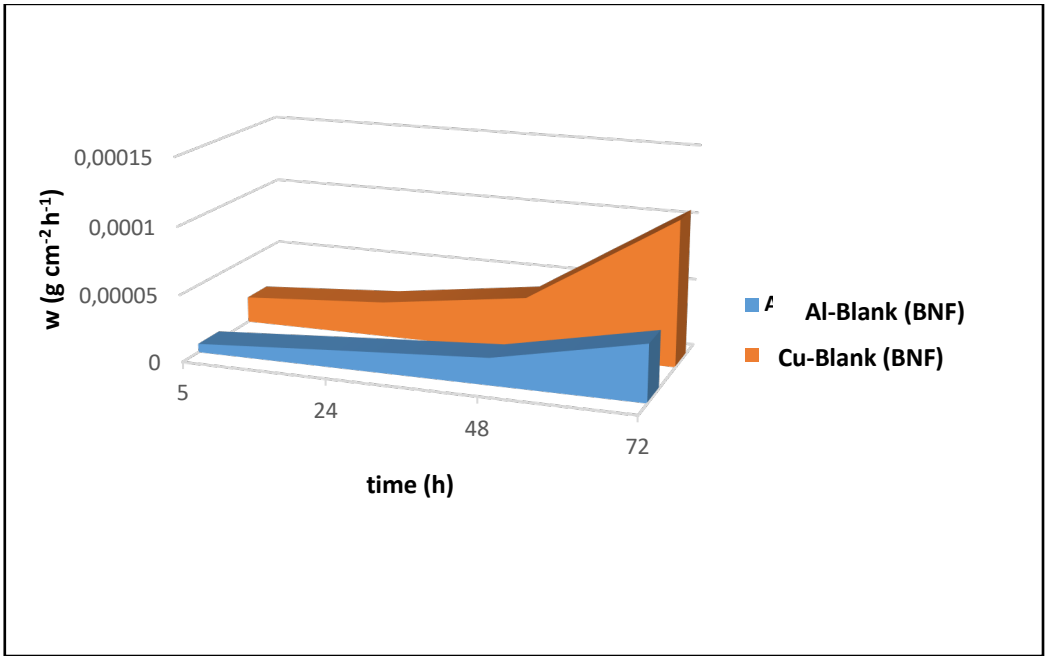

Figure 20: Evolution of the corrosion rate as a function of time in the BNF of Cu and Al

The two graphs in the figure above show an increase in the corrosion rate during the different contact times of aluminum and copper with unfiltered biogas. A comparison of the two graphs suggests that the slight increase in corrosion rate observed for copper compared to aluminum is due to the crystalline structure of each metal.

3.3.3.2 Comparative study of aluminum and copper (Cu) corrosion rates as a function of time (t) in filtered biogas (BF)

Figure 21: below shows the variation of aluminum and copper corrosion rates as a function of time in filtered biogas. The two curves in **Figure 21** above show a decreasing trend in overall corrosion rate over the study time. Both curves show a drop-in corrosion rate from 5 h to 24 h, before remaining almost constant between 24 h and 72 h. Aluminium's corrosion rate in this environment is much lower than that of copper. This can be explained by the fact that aluminum's protective layer is much more effective in this environment than that of copper.

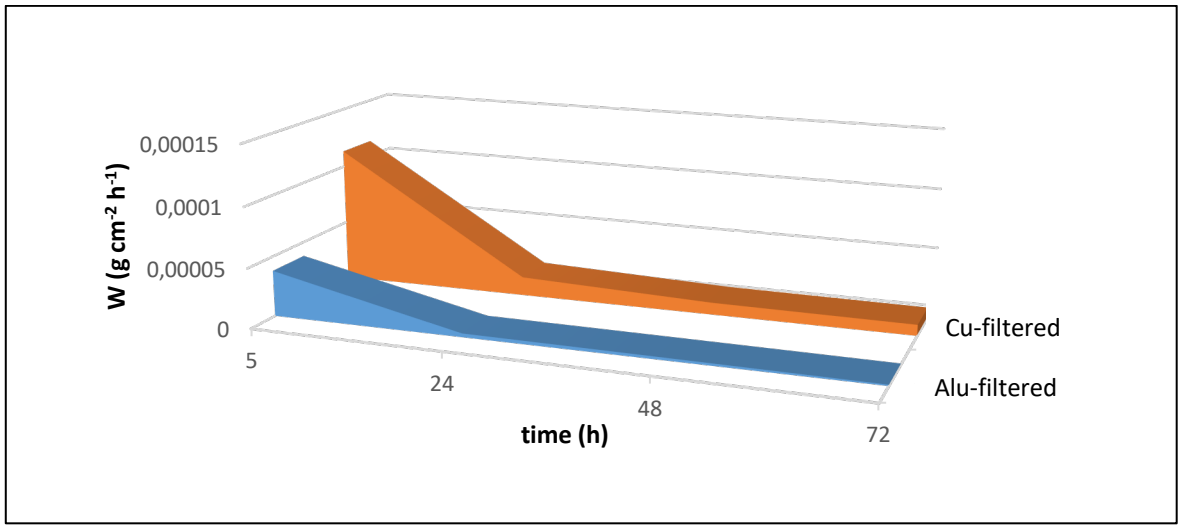

Figure 21*:* Corrosion rate vs. time in filtered biogas (BF) for the metals copper and aluminum.

3.3.4 Study of induced protective power (IPP)

3.3.4.1 Study of the protective power induced by filtration as a function of time (case of aluminum)

Figure 22 below shows the evolution of filtration-induced aluminum protective power as a function of time in filtered biogas.

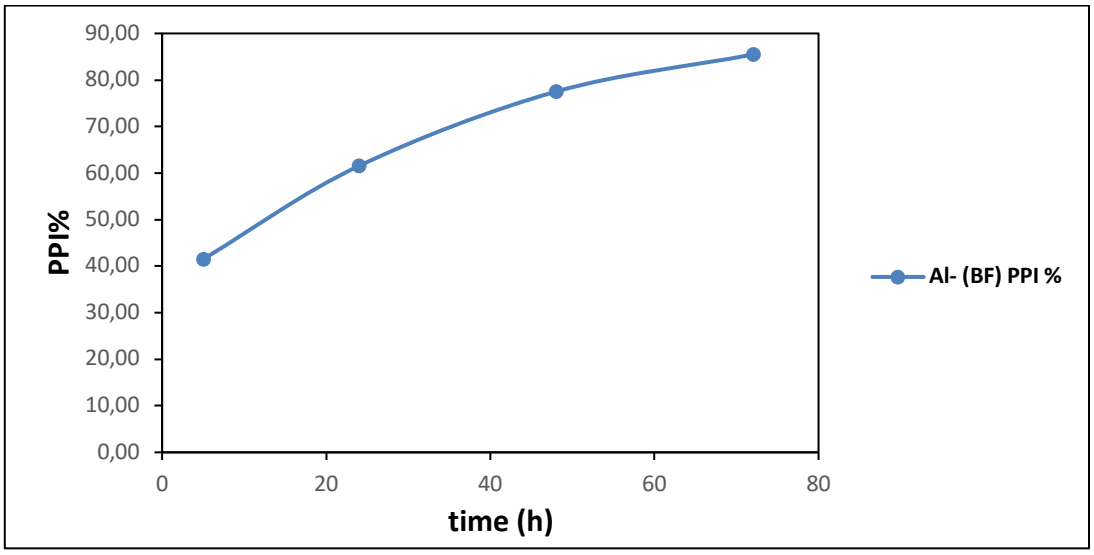

Figure 22: Evolution of the protective power induced in filtered biogas (case of aluminum).

Figure 22 above also shows that the protective power induced by filtration increases over time from 41.50% to 85.47%. This would indicate the presence of a physical barrier that gradually expands,

resulting in a high degree of coverage of the copper metal surface by traces of activated carbon. In this way, a large part of our metal would be isolated from the aggressive environment (Ikeuba *et al.,* 2019). Consequently, CACGP activated carbon would have good protective properties for aluminum.

3.3.4.2 Study of the protective power induced by copper filtration as a function of time (copper)

Figure 23 below shows the evolution of filtration-induced protective power as a function of time in filtered biogas. Analysis of this figure 23 shows that the protective power (i.e. the rate of surface coverage) increases over time from 40 to 82.63%, indicating the presence of a physical barrier that gradually expands. As a result, the copper surface will be increasingly covered by traces of charcoal. In this way, a large part of our metal would be isolated from the aggressive environment environment (Ikeuba *et al.,* 2019). As a result, CACGP activated carbon has a good protective effect on copper in filtered biogas.

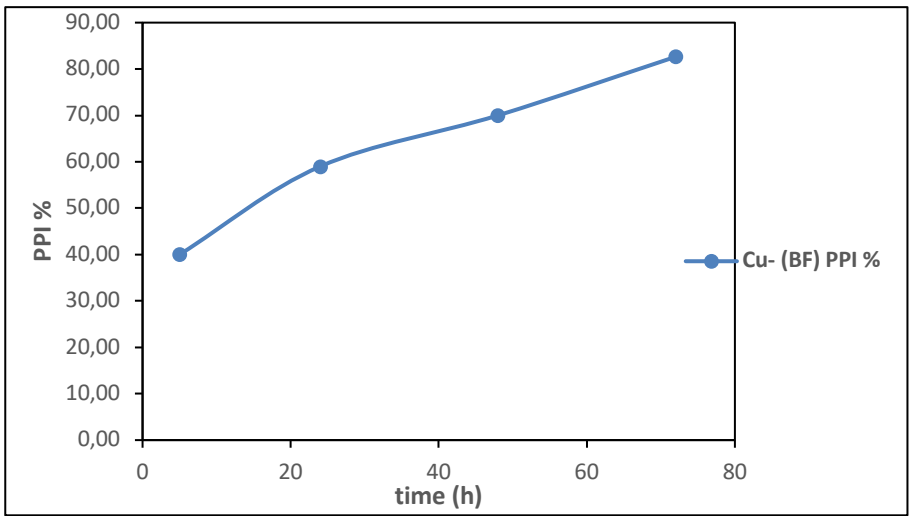

Figure 23: Evolution of induced protective power in filtered biogas (case of copper)

3.3.5 Comparative study of induced protective power for copper and aluminum as a function of time in filtered biogas.

Figure 24 below shows the evolution of the induced protective powers of aluminum and copper as a function of time in filtered biogas (BF).

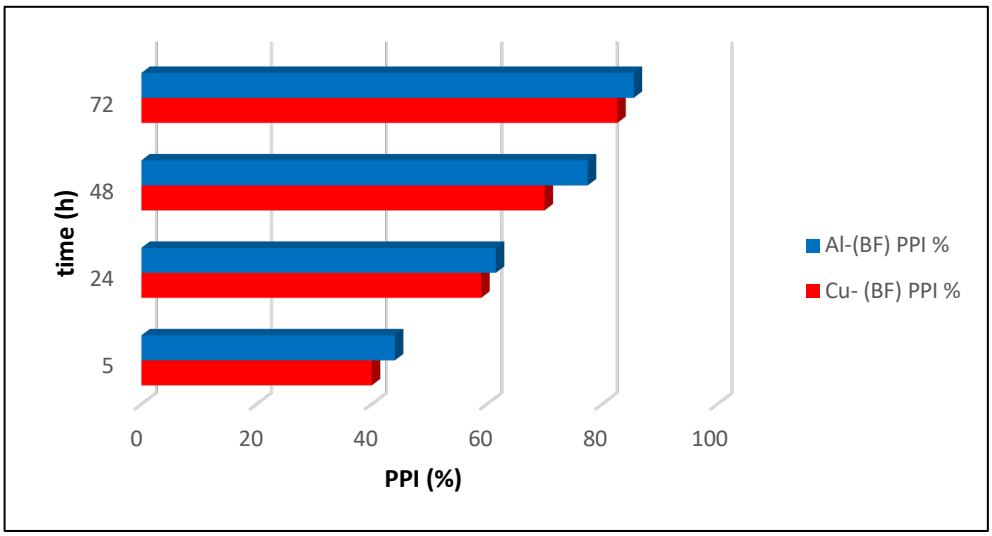

Figure 24. Time-dependent evolution of the induced protective powers of aluminum and copper in filtered biogas (BF).

Analysis of this figure shows that for all study times, the induced protective power of aluminum in filtered biogas is greater than that of copper in filtered biogas. This could be explained by the different crystalline structures of the two metals aluminum and copper. As a result, aluminum is more resistant than copper to corrosion in filtered biogas. CACGP activated carbon has good protective properties.

4. GENERAL CONCLUSION

The parameters of activated carbon based on palm kernel shells, such as iodine value, yield, ash content and pH at zero loading point, were 818.505 mg/g, 41%, 4.36% and 5.0 respectively. These results indicate that the activated carbon prepared is microporous (0-2 mm), of good quality and lightweight. Furthermore, the activated carbon samples prepared have a H_2S removal efficiency (RE), during the working time (10 h), of over 90% for the 30 g filtration column used with H_2S output concentrations below 10 ppm, which is the tolerance threshold for prolonged exposure. Activated carbon based on palm kernel shells can therefore be used to remove hydrogen sulfide from biogas.

The induced protective power values (i.e. the surface coverage rate) for aluminum and copper in filtered biogas are 85.47% and 82.63% respectively. CACGP activated carbon has good protective properties.

The protective layer of aluminum is much more effective in this environment than that of copper. As a result, aluminum is more resistant than copper to corrosion in biogas.

REFERENCES

Abdirakhimov, M., Al-rashed, M. H., et Wójcik, J. (2022). Recent Attempts on the Removal of H_2S from Various Gas Mixtures Using Zeolites and Waste-Based Adsorbents; *Energies,* 15, no 15, 5391.

Abuiboto, M. C. N., Avom, J., Mpon, R., (2016). Properties of activated carbon prepared from residues of African pearwood (Baillonella toxisperma Pierre) and tested by iodine adsorption from aqueous solution. Revue des Sciences de l'Eau: *Journal of Water Science*, 29, no 1, 51-60.

Ali, M. (2021). Etude expérimentale et modélisation de la combustion de biocombustibles solides issus de la biomasse lignocellulosique sur lit fixe. *Thèse de doctorat*. Université de Monastir.

Asmara, Y. P., (2018). The roles of H_2S gas in behavior of carbon steel corrosion in oil and gas environment; a review; *Jurnal Teknik Mesin (JTM)*, 7, no 1, 37-43.

Balogoun, C. K., BAWA, M. L., Osseni, S., (2015). Préparation des charbons actifs par voie chimique à l'acide phosphorique à base de coque de noix de coco. *International Journal of Biological and Chemical Sciences,* 9, no 1, 563-580.

Benhamed, Imane. (2015). Amélioration par ajout d'un métal de transition de la régénération in situ d'un charbon actif par oxydation catalytique. *Thèse de doctorat.*

Benhamed, I., Barthe, L., Kessas, R., Julcour, C., & Delmas, H. (2016). Effect of transition metal impregnation on oxidative regeneration of activated carbon by catalytic wet air oxidation. *Applied Catalysis B: Environmental,* 187, 228-237.

Coelho, C., Oliveira, Ana S., Pereira, M. R., (2006). The influence of activated carbon surface properties on the adsorption of the herbicide molinate and the bio-regeneration of the adsorbent. *Journal of hazardous materials,* 138, no 2, 343-349.

Demey, H., Vincent, T., Guibal, E. (2018). A novel algal-based sorbent for heavy metal removal; *Chemical Engineering Journal,* 332, 582-595.

Dustin, H. (1934). Considérations sur les méthodes d'essai des aciers à hautes températures. *Revue de Métallurgie*, 31, no 9, 409-420.

Ehouman, A. D., Bamba, A., Toure, H., Adou, E., Kouakou, A. R., Mariko, K., Dja, A., Niamien, P.,Yao, B. (2023). Inhibition Effect of Tenoxicam on Copper Corrosion in HNO3: Experimental Study and DFT. American Journal of *Materials Science and Engineeringvol.* 11, no 1, 7-15.

Ehouman,A. D., TINDO, S. (2023). Removal of Hydrogen Sulphide from Biogas by Activated Carbon Based on Borassus Aethiopum (Ivory Coast). *An International Peer Review E-3 Journal of Sciences*, JCBPS; Section D; 13, No. 1, 041-050.

EL Houari, A. (2018), Production et élimination des sulfures produits lors de la biométhanisation de boues de station de traitement des eaux usées domestiques: Procédés biologiques de sulfooxydation par des thiobacilles anaérobies facultatifs (projet SULFOX). *Thèse de doctorat. Pau.*

El Mouaden K., El Ibrahimi B., Oukhrib R., Bazzi L., Hammouti B., Jbara O., Tara A., Chauhan D. S., Quraishi M.A. (2018) Chitosan polymer as a green corrosion inhibitor for copper in sulfide-containing synthetic seawater, *International Journal of Biological Macromolecules,* 119, 1311-1323

Fontenelle, M., Alves, H. J., Monteiro, M. R., Silvia, M. H., Carlos, A., Della, R., Eder, L. P. (2017). Evaluation of corrosion caused by the use of in natura biogas in steam generator boilers of carbon steel structural elements. *Materials Research*, 20, 725-735.

Frank T. K. (2012). Etude des performances des charbons actifs préparés à partir de biomasses tropicales pour l'élimination du chrome et diuron en milieu aqueux. *Mémoire de master en environnement option assainissement. 2iE, Burkina Faso*,

Gbangbo, K. R., Kouakou, A. R., Ehouman, A. D., Yao, B., Goli Lou, G. V. E., Gnaboa, Z., & Bailly, G. C. (2023). Influence of water content on hydrogen sulfide adsorption in biogas purification with Musa paradisiaca biochar. *Chemistry Africa,* 6(2), 657-665.

Hu, Z. et Srinivasan, M. P. (1999). Preparation of high-surface-area activated carbons from coconut shell. *Microporous and Mesoporous Materials,* 27, no 1, 11-18.

Ikeuba, A. I. et OKAFOR, P. C. (2019). Green corrosion protection for mild steel in acidic media: saponins and crude extracts of *Gongronema latifolium*. *Pigment & Resin Technology,* 48, no 1, 57-64.

Kaiser, F., Diepolder, M., Eder, J., Hartmann, S., Prestele, H., Gerlach, R., Gronauer, A. (2004). Biogaserträge verschiedener nachwachsender *Rohstoffe; Landtechnik,* 59 no 4, 224-225.

Koné, H., Assémian A. S., Tiho, T., (2022). *Borassus aethiopum* activated carbon prepared for nitrate ions removal. *Journal of Applied Water Engineering and Researchvol*. 10, no 1, 64-77.

Kouakou, A. R., Ehouman, A. D., Konan, A. T. S, Kouadio, N. J., Kra, D. O., Adou, K. E., Gbangbo, K. R., Ekou, T., (2022). Élimination du sulfure d'hydrogène du biogaz par l'*Acacia Auriculea formis* Charbon actif. Science *Journal of Chemistry*. 10, no 5, 170-176.

Kougias, P. G. et Angelidaki, I., (2018). Biogas and its opportunities-A review; *Frontiers of Environmental Science & Engineering, 12, 1-12.*

Laine, J., Calafat, A. (1989). Preparation and characterization of activated carbons from *coconut shell* impregnated with phosphoric acid. *Carbon,* 27, no 2, 191-195.

Mao, D., Griffin, J. M., Dawson, R., Alasdair, F. G. S., Gupta, Nuno B., (2021). Porous materials for low-temperature H_2S-removal in fuel cell applications. *Separation and Purification Technology,* 277, 119426.

Moletta, R., (2011). Technologies de la méthanisation de la biomasse Déchets ménagers et agricoles. *La méthanisation, in French,* p. 177.

Nikiema, M., Sawadogo, J. B., Somda, M. K. (2015). Optimisation de la production de biométhane à partir des déchets organiques municipaux. *International Journal of Biological and Chemical Sciences,* 9, no 5, 2743-2756.

Nyamukamba, P., Mukumba, P., Chikukwa, (2022). Evernice Shelter, et al. Hydrogen Sulphide removal from biogas: A review of the upgrading techniques and mechanisms involved. *International Journal of Renewable Energy Research (IJRER)*, 12, no 1, 557-568.

Koné, H., Kouassi, K. E., Assémian, A. S. (2021). Investigation of breakthrough point variation using a semi-industrial prototype packed with low-cost activated carbon for water purification. *Journal of Materials and Environmental Science, vol.* 12, p. 224-243.

Koné, H., Assémian, A. S., Tiho, T., Adouby, K., Yao, K. B., & Drogui, P. (2022). *Borassus aethiopum* activated carbon prepared for nitrate ions removal. *Journal of Applied Water Engineering and Research,* 10(1), 64-77.

Prahas, D., Kartika, Y., Indraswati, N. (2008). Activated carbon from jackfruit peel waste by H3PO4 chemical activation: Pore structure and surface chemistry characterization. *Chemical Engineering Journal*, vol. 140, no 1-3, p. 32-42.

Promnuan, K., Sompong, O. T. (2017). Biological hydrogen sulfide and sulfate removal from rubber smoked sheet wastewater for enhanced biogas production. *Energy Procedia,* vol. 138, p. 569-574.

Rodrigue, K. A., Donatien, E. A., Sylvie, K. A. Tindo, (2022). Removal of Hydrogen Sulfide from Biogas by the *Acacia Auriculeaformis Activated Carbon. Science,* 10, no 5, 170-176.

Sawalha, H., Maghalseh, M., Qutaina, J., Junaidi, K., & Rene, E. R. (2020). Removal of hydrogen sulfide from biogas using activated carbon synthesized from different locally available biomass wastes-a case study from Palestine; *Bioengineered,* 11, no 1, 607-618.

Search, N. & Out, L. (2012). Standard test method for Brinell hardness of metallic materials. *ASTM International*, p. 1-36.

Shang, G., Li, Q., Liu, L., Chen, P., & Huang, X. (2016). Adsorption of hydrogen sulfide by biochars derived from pyrolysis of different agricultural/forestry wastes. *Journal of the Air & Waste Management Association*, 66(1), 8-16.

Sun, W., Pugh, D. V., Smith, S. N., Ling, S., Pacheco, J. L., & Franco, R. J. (2010). A Parametric Study Of Sour Corrosion Of Carbon Steela; *In NACE CORROSION* p. 10278

Tsassa, C., (2015). Planification de l'émergence en Côte d'Ivoire: éléments de réflexion. *In: Conférence Internationale sur l'émergence de l'Afrique, janvier.*

(2023) ; http://www.jmaterenvironsci.com